From Proceedings 1989 American Control Conference, Pittsburgh, PA
June 21-23, 1989.

FA7 - 11:45

SMALL MOTION EXPERIMENTS ON A LARGE FLEXIBLE ARM WITH STRAIN FEEDBACK[1]

B. S. Yuan
American Semiconductor Equipment Technologies
Woodland Hills, California

J. D. Huggins
W. J. Book
Georgia W. Woodruff School of Mechanical Engineering
Georgia Institute of Technology
Atlanta, Georgia

ABSTRACT

Initial experiments on state space feedback control of a large flexible manipulator with a parallel linkage drive are described. A linear controller using joint angle and strain measurements was designed to minimize a quadratic performance index with a prescribed stability margin. It is based on a simplified model that accounts for the constraints of the parallel linkage kinematically rather than through constraint forces. The results show substantial improvement over a simple P.D. joint control.

INTRODUCTION

A large, two link flexible manipulator designated RALF (Robotic Arm, Large and Flexible) is the subject of modeling and control research at Georgia Institute of Technology. It is hydraulically actuated with the second joint powered through a parallelogram linkage. This drive linkage is representative of drives found in many large articulated arms. It allows the substantial weight of the actuators to be located near the base hence reducing the weight that must be supported and the inertia that must be moved. A parallelogram arrangement allows the drive for the second joint to carry some of the bending load on link 1 as well. Most control researchers have avoided this practical configuration, especially when the links are flexible for the more tractable direct drive, serial link problem. The direct drive concept has not been employed for large articulated arms in earth's gravity and may never be practical in that application.

The difficulty of research with the parallelogram mechanism is the conceptual difficulty of modeling a system with nonlinear large motion dynamics, distributed flexibility, and constraints of closed kinematic chains. One valuable contribution of the research described here is the determination of a simple yet adequate model for RALF and other arms of this type. The second contribution is the analytical development and experimental testing of simple linear state space controllers.

1This work was partially supported through NASA Grant NAG1-623 and the Computer Integrated Manufacturing Systems Program at the Georgia Institute of Technology.

DYNAMIC MODELING

Dynamic models for RALF have been developed and compared to experiment as reported in Lee, et.al. [1]. That model included an assumed modes approximation for the link deformation and algebraic constraint equations representing the closed chain topology of the parallel actuating link. A simpler model is used here as the result of two key assumptions. First, the kinematics of the deflection assumed allows no beam extension. Hence the distances between pin joints in the parallelogram remains constant and deflection of the lower or actuating link causes no rotation in the upper link. The thicker cross section of the upper link between the pins (points E and F in the schematic of Fig. 1) makes reasonable the second assumption: rigidity in that segment of the upper link. Consequently, the segment E-F remains parallel to the same line while deflections rotate the lower link. This is in sharp contrast to serial link arms. These facts will now be incorporated into the description of the arm's motion.

As proposed in Book [2], kinematics of serial flexible arms is readily described by 4x4 transformation matrices. In particular, consider the two link arm of Fig. 1. The transformation matrix between link-fixed coordinates and base coordinates is composed of joint transformation matrices A_i and flexible link transformation coordinates E_i. The transformation to a point located a distance l_2 along the beam from the second joint is

$$T_2 = A_1 E_1 A_2 E_2. \qquad (1)$$

The point on the second link is located at ${}^2r_2$ in the link-fixed frame or at point r_2 in the base frame, where

$$r_2 = T_2\,{}^2r_2. \qquad (2)$$

The constraints of the parallelogram mechanism on link two can be readily incorporated in the rotation matrix of E_1. In general (for small deflections)

$$E_i = \sum_{j=1}^{m_i} \delta_{ij} \begin{bmatrix} 0 & -\theta_{zij} & \theta_{yij} & u_{ij} \\ \theta_{zij} & 0 & -\theta_{xij} & v_{ij} \\ -\theta_{yij} & \theta_{xij} & 0 & w_{ij} \\ 0 & 0 & 0 & 0 \end{bmatrix} + \begin{bmatrix} 1 & 0 & 0 & 0 \\ 0 & 1 & 0 & 0 \\ 0 & 0 & 1. & l_i \\ 0 & 0 & 0 & 0 \end{bmatrix}$$

where

δ_{ij} is the time varying amplitude of the shape function,

u_{ij}, v_{ij} and w_{ij} are the x, y, and z components, respectively, of the shape functions,

θ_{xij}, θ_{yij}, and θ_{zij} are the small rotations of the body-fixed coordinate system at the point of interest,

m_i is the number of shape functions needed to represent the flexible kinematics to the degree of accuracy needed, and l_i is the distance to the point of interest along the links neutral axis, which is L_i, the length of the link, when the point at r_k is not on link i.

In the special case at hand the rotations θ_{x1j}, θ_{y1j}, and θ_{z1j} are zero as seen by link two. Only translations of the tip of link one are experienced by link two.

It should be made clear that the model still accounts for rotations of the beams in the equations, but that the kinematic constraints prevent those rotations from propagating to link two in the ideal case of the joint rotational axis on the beam neutral axis. Comparing the drawing and the schematic of Fig. 1 will show a substantial offset in the laboratory hardware. This is an additional approximation in the dynamic model.

Given the above description of the arm kinematics, 8.4 the derivation of the dynamic equations of motion can proceed using Lagrange's equations substantially the same as described in Book [2]. The method shown here for two links can be extended to additional parallelogram actuated links.

It is desirable to account for the cumulative compliance of the actuating link, pin joints, and hydraulic fluid in the actuator. Including a simple massless spring effectively accomplishes this. One end of the spring is attached to the second link and the spring compression is prescribed by the actuator displacement. Lagrange's equations can accommodate this model simply with an additional term in the system kinetic energy. The method employed here differs somewhat, however. The actuator force, instead of displacement, is chosen as the input. The force acting through a massless spring is instantaneously felt by the link and the spring is of no direct consequence. The actuator spring is of consequence in the selection of assumed mode shapes for the links, however, as described below.

The transformation matrix E_i contains deflection displacements and rotations as a function of position l_i along the link. The spatial dependence of these deflections, their shape, is theoretically required only to meet modest restrictions at the link boundaries in an infinite order model. A finite element approach was used in this research to determine the shapes from detailed models of the link geometry and material properties. Of crucial importance to the accuracy of a low order model are the boundary conditions applied in deriving the shapes. Equivalent springs were used to represent the actuators for both links. Equivalent masses and inertias were also placed at the end of each link, yielding boundary conditions at 3 points on each link: at each end and where pinned in the middle. At these points on

Link 1: pinned, spring, inertia
Link 2: pinned, spring, mass

The final nonlinear equations derived by Lagrangian or other equivalent method is of the form

$$M(x)\,\ddot{x} + H(x,\dot{x})\,\dot{x} + K\,x = Q \qquad (4)$$

where

x is a vector containing the joint angles θ_i and the deflection amplitudes δ_{ij}

M is the inertia matrix

$H(x,\dot{x})$ contains the nonlinear velocity dependent functions

K is a spring constant matrix

Q is a vector of actuator torques.

CONTROL

Using the model developed in above, an LQR (Linear Quadratic Regulator) controller was developed for RALF. The points about which the model was linearized are $\theta_1 = 0°$ and $\theta_2 = 90°$. The LQR controller utilizes strain feedback from strain gages mounted near the base of the links to control vibrations of the links.

The linearized form of the equations of motion is:

$$[M]\,\{\ddot{\bar{x}}\} + [K]\{\bar{x}\} = \{Q\}$$

where $\bar{x}$, M, K, and Q are given by:

$$\{\bar{x}\}=\begin{Bmatrix}\bar{\theta}_1\\ \delta_1\\ \bar{\theta}_2\\ \delta_2\end{Bmatrix};\quad [M]=\begin{bmatrix}1949.92 & 12.47 & 317.74 & 2.365\\ 12.47 & .0998 & 0 & 0\\ 317.74 & 0 & 317.74 & 2.365\\ 2.365 & 0 & 2.365 & 1.786\ E\text{-}2\end{bmatrix}$$

$$\{Q\}=\begin{Bmatrix}\tau_1\\ 0\\ \tau_2\\ 0\end{Bmatrix};\quad [K]=\begin{bmatrix}6124860 & 0 & 0 & 0\\ 0 & 157.02 & 0 & 0\\ 0 & 0 & 1814400 & 0\\ 0 & 0 & 0 & 60.94\end{bmatrix}$$

Note that: $\theta_1 = \theta_{10} + \bar{\theta}_1$
$\theta_2 = \theta_{20} + \bar{\theta}_2$

where $\theta_{10} = 0°$ and $\theta_{20} = 90°$. See Figure 24.

writing this in state space form yields:

$$\frac{d}{dt}[X] = \frac{d}{dt}\begin{bmatrix}\bar{x}\\ \dot{x}\end{bmatrix} = \begin{bmatrix}0 & I\\ -M^{-1}K & 0\end{bmatrix}\begin{Bmatrix}\bar{x}\\ \dot{x}\end{Bmatrix} + \begin{bmatrix}0\\ M^{-1}Q\end{bmatrix} u$$

For this LQR controller the following quadratic cost criteria was used to obtain a prescribed degree of stability:

$$PI = \frac{1}{2}\int_0^t e^{2\alpha t}\,[X^T PX + u^T Ru]\,dt$$

with α, P, and R given by:

$$\alpha = 2$$

$$R = 1.E\text{-}5\begin{bmatrix}1 & 0\\ 0 & 1\end{bmatrix}$$

$$P = \begin{bmatrix}1E11 & 0 & 0 & \cdots & 0\\ 0 & 1 & & & \\ & 1E11 & & & \\ & & 1 & & \\ & & & 1 & \\ 0 & & & & 1\end{bmatrix}$$

and $u = -F(x - x_r)$ where x_r is the reference state variable. Notice the large values in the [Q] matrix corresponding to the joint position variables. Two factors influenced these numbers. First, the system model was derived using inches as the unit of length. This resulted in very small numbers when $[M]^{-1}$ is formed. Secondly, the hydraulics actuators are very stiff and inherently have a high gain. The large numbers in the [P] matrix compensate for these factors. The small numbers in the [R] matrix also resulted because of the system of units used in deriving the model.

Using a controller design software, CTRL-C, the LQR feedback gains were found as follows:

$$F=\begin{bmatrix}2.8161E7 & 1.3518E4 & 3.1388E4 & 8.3383E3 & 2.8013E5\\ 1.5035E5 & -4.4833E3 & 3.0015E7 & 1.0065E4 & 4.6735E4\\ 1138.4 & 4.483E4 & 248.226 & & \\ -12.9825 & 7.7616E4 & 268.2405 & & \end{bmatrix}$$

This yields a state space system of the form:

$$\dot{X} = (A - BF)X + BX_R$$

It should be mentioned here that the feedback gains found by solving the LQR equations do not result in absolute values. What is important is the relative magnitude of the gains. When the controller was implemented, the gains were scaled to match the physical capabilities of the system.

The controller for RALF was then implemented on a Microvax II computer with a sampling rate of 8 milliseconds. The language used is FORTRAN. All path planning is calculated before movement starts. The following graphs show the results of the LQR controller compared to a controller that does not utilize strain feedback, ie., a controller using joint position feedback only. The LQR regulator uses differentiation and filtering to estimate all rates.

Figure 3 is a plot of the strain in the lower link when the manipulator is subjected to a step input. Figure 3-a. shows the strain in the lower link when the controller uses joint position feedback only. Figure 3-b. is a graph of the strain in the lower link when subjected to the same input but using the LQR controller with strain feedback instead. As can be seen in Fig. 3-b., the vibration amplitude in the lower link is reduced much more rapidly when the LQR controller is used.

Figure 4-a. shows the strain in the lower link when the controller uses joint position feedback only. Figure 4-b. is a graph of the strain in the lower link when subjected to the same input but using the LQR controller with strain feedback instead. Again the vibration amplitude is reduced much more quickly when the LQR controller incorporating strain feedback is used.

Figure 5-a. shows the strain in the lower link in response to a disturbance to the manipulator's structure. In this case, the manipulator's position is being maintained by the controller that uses joint position feedback only. Figure 5-b. shows a graph of the strain in the lower link when subjected to the same disturbance when using the LQR controller to maintain the manipulator's position. Much better disturbance rejection is seen in Fig. 5-b. than in Fig. 5-a.

SUMMARY AND FUTURE WORK

It is seen from these experiments that a suitable controller utilizing strain information from the links can

successfully damp out the vibration in the manipulator. The LQR controller is a good example of these. Since the structure's dynamics are non-linear, a better controller might be one that incorporates some nonlinearities and adapts to changes in configuration. Work on this aspect is underway.

REFERENCES

1. Lee, J. W., Huggins, J. D., and Book, W. J., "Experimental Verification of a Large Flexible Manipulator," Proceedings of the 1988 American Control Conference, June 15-17, 1988, Atlanta, Georgia 1021-1028.

2. Book, W. J., "Recursive Lagrangian Dynamics of Flexible Manipulators Arm," The Int. J. of Robotics Research, Vol. 3, No. 3, 1984, pp. 87-101.

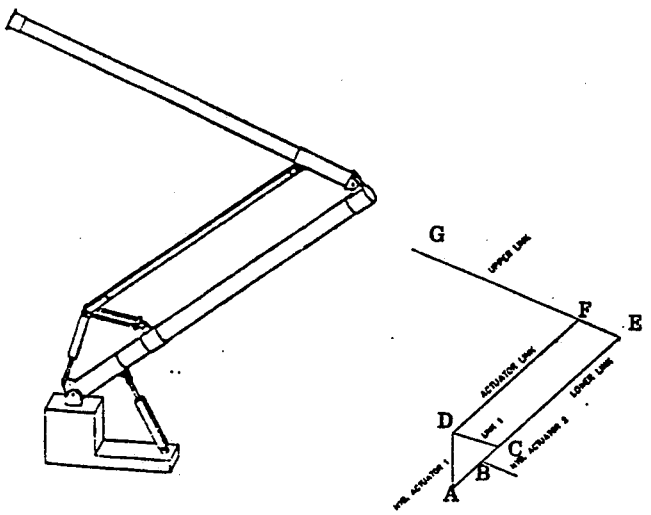

Figure 1. Robotic Arm Large and Flexible (RALF); Actual and Idealized.

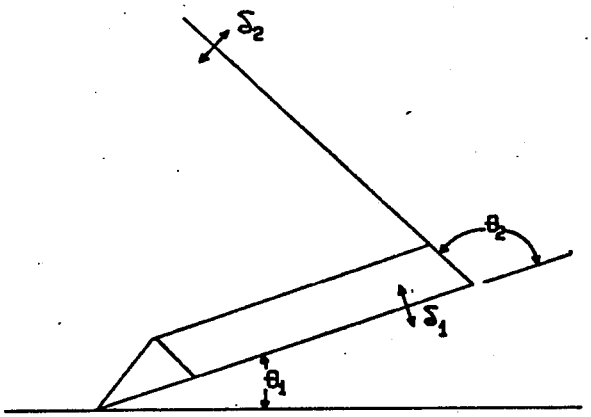

Figure 2. Variables in RALF Model

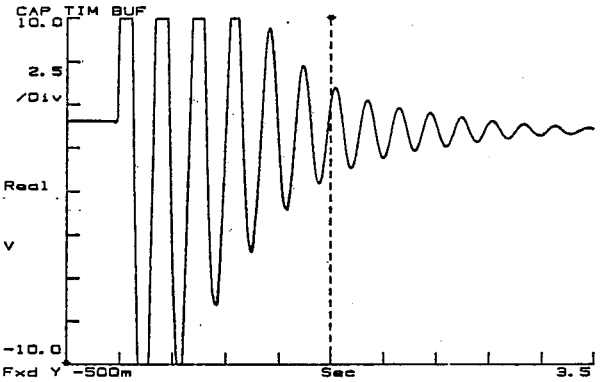

Figure 3a. Lower Link Strain for Joint P.D. Control, Step Input.

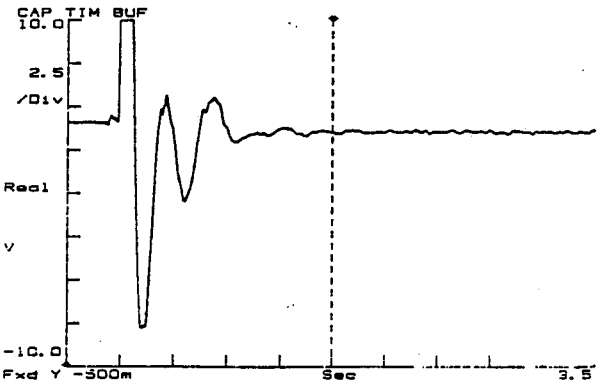

Figure 3b. Lower Link Strain for Strain Feedback LQR, Step Input.

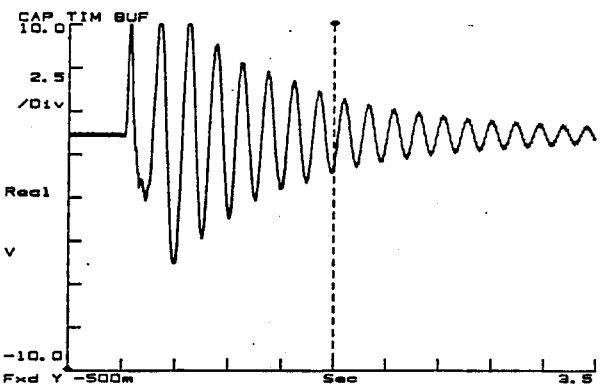

Figure 4a. Lower Link Strain for Joint P.D. Control, Step Input.